

# The abundances of the elements in the solar photosphere – VIII. Revised abundances of carbon, nitrogen and oxygen

David L. Lambert *Department of Astronomy, University of Texas, Austin, Texas*

Received 1977 April 5; in original form 1976 December 21

**Summary.** A comprehensive analysis of atomic and molecular lines provides the following recommended solar photospheric abundances for carbon, nitrogen and oxygen

$$\log \epsilon(\text{C}) = 8.67, \log \epsilon(\text{N}) = 7.99 \text{ and } \log \epsilon(\text{O}) = 8.92$$

on the standard scale  $\log \epsilon(\text{H}) = 12.00$ . An uncertainty of  $\pm 0.10$  dex is indicated.

Primary abundance indicators include the [C I]  $\lambda$  8727 line, the CH A-X and C<sub>2</sub> Swan systems, the N I lines and the [O I]  $\lambda\lambda$  6300, 6363 lines.

## 1 Introduction

All accessible atomic and molecular signatures of carbon, nitrogen and oxygen are integrated in this comprehensive updating of an earlier paper in this series (Lambert 1968). The reasons for presenting another CNO abundance study are stated briefly in this Introduction.

External interest in accurate CNO abundances remains high: the solar abundances are a primary source for the entry in cosmic abundance tables (*cf.* Cameron 1973); depletion of these elements in the interstellar gas is measured with reference to the solar abundance in the absence of reliable abundances from younger objects (OB stars, H II regions); accurate photospheric abundances are required for an assessment of interesting diffusion effects in the corona and solar wind for which accurate abundances are becoming available.

Significant progress on the thorny problem of  $f$  values for atomic and molecular lines has been reported in recent years. Highlights include exciting new experimental results on forbidden lines, the application of pulsed dye lasers and the introduction of the high-frequency deflection technique for the precise measurement of radiative lifetimes for individual rotational states. Although the progress since the 1968 paper has been dramatic, lacunae exist and a subsidiary purpose of this paper is to spotlight the critical gaps.

Little attention in recent years appears to have been directed at the N and O abundances. The C abundance has been the focus of several new analyses. In recent papers (Mount & Linsky 1975a and references therein), a suggestion is promoted that the C abundance should be reduced by about 0.2 dex from the 1968 value. The present discussion of the prime abundance sources shows that this correction factor is incorrect; the new abundance is 0.12 dex higher than in 1968.

## 2 Atomic and molecular lines of C, N and O

### 2.1 THE C I SPECTRUM

#### 2.1.1 The permitted lines

Although C I lines are plentiful in the photospheric spectrum, few lines can be given a high priority for inclusion in an abundance analysis. The ideal line is weak and unblended with an accurate  $f$  value and formed in local thermodynamic equilibrium (LTE). Weak solar C I lines exist. Transition arrays with  $\Delta n = n' - n'' \geq 1$  provide most of the weak lines ( $n$  = the principal quantum number, upper and lower states are denoted by single and double primes). Unfortunately, an  $f$ -value calculation for many of these arrays is beset with the difficulty that the Coulomb radial integrals experience considerable cancellation (Lambert 1968). A further difficulty is that LS-coupling is not widely applicable to the C I terms; significant departures from the Landé interval rule are evident except for the  $2s^2 3p 3s$  and  $2s^2 2p 3p$  configurations. Since intermediate coupling calculations are not yet available, use of theoretical (ca + LS)  $f$  values is restricted to the  $3s-3p$  array. Scaled Thomas–Fermi wave functions provide radial integrals (van Rensbergen 1970) for the  $3s-3p$  array that differ by only 0.03 dex from the Coulomb approximation values. These problems with the  $f$  values of the weak solar lines require an inspection of the experimental work.

Analysis of emission line intensities from a stabilized arc (Richter 1958) gave absolute transition probabilities for several C I multiplets. Comparison with the theoretical  $f$  values shows Richter's values for the  $3s-3p$  array are too small by 0.15 dex. This array provides few weak solar lines; the strong lines (say  $W_\lambda > 120 \text{ m}\text{\AA}$ ) are ejected from the abundance analysis because the collisional damping constants are uncertain. Additional weak infrared lines from the  $3p-4s$  array are included with  $f$  values taken from Richter and increased by 0.15 dex.

$f$  values for weak lines in the visible spectrum are obtainable from the shock tube study reported by Miller *et al.* (1974) who gave results for 12 multiplets with errors of  $\pm 12$  to  $\pm 40$  per cent. Their comparison with other experimental results shows fair agreement. For five multiplets in common, Richter's  $f$  values average 0.06 dex smaller; the difference is in the same sense as the above  $3s-3p$  comparison. An arc-plasma emission line measurement

Table 1. Permitted C I lines.

Transition	$J''-J'$	$\lambda$ (Å)	$\chi$ (eV)	$\log gf$	Ref.*	$W_\lambda$ (mÅ)
$3s \ ^3P^0-3p \ ^3D$	2-1	10753.99	7.49	-1.59	a	45
$\ ^3P^0-^3S$	0-1	9603.03	7.48	-0.94	a	95
$\ ^1P^0-^1S$	1-0	8335.15	7.68	-0.42	a	108
$3p \ ^3D-4s \ ^3P^0$	3-2	11895.75	8.65	0.04	b	108
	2-1	11892.91	8.64	-0.23	b	80
	2-2	11848.73	8.64	-0.71	b	42
	1-0	11879.59	8.64	-0.58	b	50
	1-1	11862.99	8.64	-0.71	b	46
$3s \ ^3P^0-4p \ ^3P$	2-1	4775.91	7.49	-2.16	c	19
$\ ^1P^0-^1P$	1-1	5380.34	7.68	-1.69	c	26
$\ ^1P^0-^1D$	1-2	5052.17	7.68	-1.51	c	40

\* References to the  $f$  values:

- Theoretical (Coulomb approximation and LS coupling).
- Scaled from Richter (1958) – see text.
- Miller *et al.* (1974).

(Stuck & Wende 1974) gave a transition probability  $A = (1.4 \pm 0.3)10^6 \text{ s}^{-1}$  for the 5052 Å line which compares favourably with  $A = (1.6 \pm 0.2)10^6 \text{ s}^{-1}$  by Miller *et al.* Miller *et al.* values are adopted here for the 4775, 5052 and 5380 Å lines. The 6587 Å line appears unblended but the derived abundance is a factor of 3 larger than the mean from other C I lines.

The adopted C I line list is given in Table 1. The centre-of-disk equivalent widths ( $W_\lambda$ ) for the infrared lines are taken from Lambert (1968). When possible,  $W_\lambda$  for the visible lines were measured off the new Liège spectra (Delbouille, Neven & Roland 1973). Additional weak lines are available especially in the infrared but reliable  $f$  values are presently unavailable.

### 2.1.2 The [C I] line at 8727 Å

The forbidden transition  $2p^2\ ^1D_2 - 2p^2\ ^1S_0$  at  $\lambda_{\text{air}} = 8727.126$  Å (Moore 1970) was identified first by Lambert & Swings (1967a), whose equivalent width ( $W_\lambda = 6.5$  mÅ) is adopted. No other [C I] lines are detectable in the Sun. The 8727 Å line is an important abundance indicator; it is weak with a reliable  $f$  value and LTE line formation appears guaranteed.

The  $f$  value is provided by recent theoretical calculations. Nicolaides & Sinanoğlu (1973) give a transition probability  $A = 0.548 \text{ s}^{-1}$ . Nussbaumer (1971) gives  $A = 0.521 \text{ s}^{-1}$ . These independent calculations are similar in that both advance upon the independent electron approximation and allow for the ‘electron correlation’ (Nicolaides & Sinanoğlu) or the ‘configuration interaction’ (Nussbaumer). The differences in the theories are discussed by Schaeffer (1972). We shall adopt a straight mean  $A = 0.535 \text{ s}^{-1}$  or  $\log gf = -8.21$ .

## 2.2 THE NI SPECTRUM

The NI line list (Table 2) adopted in 1968 was further refined by an examination of low-noise photoelectric spectra obtained at Kitt Peak National Observatory and kindly supplied by L. Testerman. Most NI lines are blended with weak CN lines. The CN contribution was estimated from other CN lines in the spectra. Table 2 gives the equivalent widths of the NI and CN components as  $W_\lambda(\text{NI})$  and  $W_\lambda(\text{CN})$  respectively; the observed equivalent width is the sum of the two values.

The  $f$  values for the solar NI lines are taken to be the theoretical values based upon Coulomb approximation radial integrals and LS-coupling line strengths. Remarkably few

Table 2. Permitted NI lines.

Transition	$J'' - J'$	$\lambda$ (Å)	$\chi$ (eV)	$\log gf$	$W_\lambda$ (NI) (mÅ)	$W_\lambda$ (CN) (mÅ)
$3s\ ^4P - 3p\ ^4D^0$	$3/2 - 5/2$	8683.40	10.33	+0.11	7.19	0.90
	$5/2 - 5/2$	8718.83	10.34	-0.26	4.90	0.97
	$1/2 - 1/2$	8703.25	10.33	-0.29	3.84	2.30
$3s\ ^4P - 3p\ ^4P^0$	$5/2 - 5/2$	8216.35	10.34	+0.13	8.30	
$3s\ ^4P - 3p\ ^4S^0$	$3/2 - 3/2$	7442.29	10.33	-0.33	2.57	0.57
	$5/2 - 3/2$	7468.31	10.34	-0.16	4.60	
$3s\ ^2P - 3p\ ^2D^0$	$3/2 - 5/2$	9392.79	10.69	+0.31	7.51	2.42
$3s\ ^2P - 3p\ ^2P^0$	$1/2 - 1/2$	8594.01	10.68	-0.32	2.85	0.33
	$3/2 - 3/2$	8629.24	10.69	+0.08	4.10	1.80
	$3/2 - 1/2$	8655.89	10.69	-0.62	1.60	
$3p\ ^4P - 3d\ ^4F$	$5/2 - 7/2$	10112.48	11.76	+0.58	3.61	
	$7/2 - 9/2$	10114.64	11.76	+0.74	5.46	
	$3/2 - 5/2$	10108.89	11.75	+0.39	2.40	

experimental results are available for a comparison. In 1968, the theoretical values were compared with Richter (1961)'s results obtained using a stabilized arc; the mean difference is small for the  $3s-3p$  and  $3p-3d$  arrays with  $f(\text{Theory})/f(\text{Richter}) = 1.2$  and  $0.96$  respectively. Since the quoted measurement errors range from  $\pm 10$  to  $\pm 15$  per cent, the measurements can be taken to confirm the theoretical values to a precision of at least 20 per cent. Another check is provided by lifetime measurements reported by Desesquelles (1971). The measurements are within 10–15 per cent of the lifetimes calculated from Richter's transition probabilities. An exception is the lifetime for the  $3d^4F$  state but Desesquelles indicates that a cascading transition may be affecting his measurement.

Inspection of the N I term diagram shows configuration interaction to affect the  $3d$  terms. This promotes the suspicion that the theoretical (ca + LS)  $f$  values may be inapplicable to the  $3p-3d$  array. The solar line analysis confirms the suspicion (see Section 4.3).

Unfortunately, the forbidden lines have not been detected (Lambert & Swings 1967b); the predicted equivalent width for the centre of the disk is only  $W_\lambda \sim 0.2 \text{ m}\text{\AA}$  for the strongest line.

## 2.3 THE O I SPECTRUM

### 2.3.1 The permitted lines

Six lines from the 1968 line list are selected (Table 3). The theoretical (ca + LS)  $f$  values adopted in 1968 appear not to require revision. Little experimental work has been reported since 1968.

Goly's (1969) analysis of emission lines from a wall-stabilized cascade arc included three multiplets providing weak solar lines. With one exception, Goly's  $f$  values for six multiplets average only 0.02 dex smaller than the theoretical values with errors placed at 12–17 per cent. The exception is the 6106 Å multiplet (this is not seen in the Sun) with a measured  $f$  value about three times larger than the theoretical value. Lifetime measurements by Copeland (1971) for several of the upper states providing solar lines are in very poor agreement with the theoretical values. In this case, the measured lifetimes probably do not refer to the radiative lifetime. Goly's new results and earlier experimental results reviewed in 1968 confirm the theoretical values.

The Coulomb approximation should be reliable for these O I transitions. Thomas–Fermi wave functions provide an  $f$  value for the 7774 Å multiplet  $f = 0.975$  (van Rensbergen 1970) which is to be compared with the Coulomb approximation result  $f = 0.925$ .

### 2.3.2 The forbidden lines

The [O I] lines at 5577, 6300 and 6363 Å are of crucial importance to oxygen abundance determinations for the Sun and stars. Happily, their  $f$  values are satisfactorily determined

Table 3. Permitted O I lines.

Transition	$J'' - J'$	$\lambda$ (Å)	$\chi$ (eV)	$\log gf$	$W_\lambda$ (mÅ)
$3s^5S^0 - 3p^5P$	2–3	7771.94	9.15	0.33	80
	2–2	7774.17	9.15	0.19	70
	2–1	7775.39	9.15	–0.03	52
$3p^5P - 3d^5D^0$	3–	9265.9	10.74	0.80	31
$3p^5P - 4d^5D^0$	3–	6158.18	10.74	–0.29	5.8
$3p^5P - 4s^5S^0$	3–2	11302.28	10.74	0.03	14

and currently available results represent a considerable improvement over the 1968 selection.

The radiative lifetime of the  $2p^4^1S_0$  state was measured by Corney & Williams (1972) who reported the transition probability sum for the 5577 and 2972 Å lines  $A(5577) + A(2972) = 1.31 \pm 0.05 \text{ s}^{-1}$ . More recently, Kernahan & Pang (1975) measured the 5577 Å [O I] intensity from an inert gas–oxygen discharge and with a simultaneous measurement of the population of the  $^1S_0$  level (the self-absorption in the 1218 Å line from the  $^1S_0$  level was measured) obtained  $A = 1.06 \pm 0.32 \text{ s}^{-1}$ . They also measured the relative intensity of the 5577 and 2972 Å lines to obtain  $A(5577)/A(2972) = 23.7 \pm 2.4$ .

The best theoretical values appear to be  $A(5577) = 1.183 \text{ s}^{-1}$  (Nicolaidis & Sinanoğlu 1973) and  $A(2972) = 0.071 \text{ s}^{-1}$  (Garstang 1956) or  $A(5577) + A(2972) = 1.25$  in very good agreement with the measurement by Corney & Williams. The theoretical value for  $A(5577)$  is consistent with the measurement by Kernahan & Pang. The theoretical ratio  $A(5577)/A(2972) = 16.7$  is in slight disagreement with the above measurement. Other measurements of this ratio are  $22 \pm 2$  (LeBlanc, Oldenburg & Carleton 1966) and  $18.6 \pm 3.7$  (McConkey *et al.* 1966). The source of the discrepancy is probably the relative intensity calibration of the instrumentation between 5577 and 2972 Å; the weak 2972 Å line is a magnetic dipole transition so that the theoretical  $A$  value should be reliable.

The 6300 and 6363 Å lines are magnetic dipole transitions with very weak electric quadrupole contributions. Yamanouchi & Horie (1952) took account of the spin–orbit interaction for a single electron and the smaller spin–orbit and spin–spin interactions between electrons; they quote transition probabilities  $A(6300) = 0.00569$  and  $A(6363) = 0.00185 \text{ s}^{-1}$ . Recently, Garstang (1976, private communication) repeated the calculations including higher terms in the spin–orbit interaction and obtained  $A(6300) = 0.00595$  and  $A(6363) = 0.00187 \text{ s}^{-1}$ . These values are adopted.

Laboratory measurements (Kernahan & Pang 1975) give  $A(6300) = 0.00515$  and  $A(6363) = 0.00166 \text{ s}^{-1}$  with an uncertainty of  $\pm 25$  per cent. Other lower precision measurements are referenced by Kernahan & Pang. The agreement with theoretical values is satisfactory. Relative intensity measurements in the same experiment gave  $A(6300)/A(6363) = 0.32 \pm 0.03$  in excellent agreement with the theoretical ratio (Garstang) of 0.318.

In this analysis, the adopted  $f$  values are  $\log gf = -8.26$  (5577 Å),  $-9.75$  (6300 Å),  $-10.25$  (6363 Å) which are respectively 0.17, 0.07 and 0.09 dex smaller than the values adopted in 1968. The theoretical and experimental evidence is markedly superior to that on which the 1968  $f$  value selection was based.

Equivalent widths were measured off large-scale plots of the new Liège Atlas:  $W_\lambda = 4.55 \text{ mÅ}$  (6300 Å) and  $1.61 \text{ mÅ}$  (6363 Å). A weak CN red system line contributes to the 6363 Å line;  $W_\lambda = 0.18 \text{ mÅ}$  is predicted from a fit to (0, 0) band lines. A Ni I line may contribute to the 6300 Å line. Four reasons suggest a very small contribution from this line:

(1) The observed peak wavelength of the solar line is within 5 mÅ of the predicted [O I] wavelength and about 30 mÅ to the blue of the predicted Ni I wavelength. These predictions include the gravitational redshift (13 mÅ) but do not include a shift arising from convective motions.

(2) The solar line is highly symmetrical. On the assumption that the Ni I and [O I] lines are separated by the predicted 32 mÅ, profile analysis suggests  $W_\lambda < 0.5 \text{ mÅ}$  as a reasonable upper limit.

(3) A prediction  $W_\lambda \sim 4.6 \text{ mÅ}$  is obtained from the corrected 6363 Å line. This corresponds to  $W_\lambda \leq 0.1 \text{ mÅ}$  for the Ni I line. However, if 6363 Å were contaminated by an unidentified line, the Ni I prediction would increase. This estimate also depends on the relative  $f$  values for the two [O I] lines.

(4) If the Kurucz & Peytremann (1975)  $f$  values are adopted for the Ni I multiplet (RMT 246) an estimate of the Ni I line can be obtained from other weak lines at 6772.0 and 6666.7 Å. These suggest  $W_\lambda \sim 0.4$  mÅ for the 6300.3 Å line. However, another line at 6331.3 Å would translate to  $W_\lambda \sim 3.5$  mÅ for the 6300.3 Å. Perhaps this line is not due to Ni I. Accurate  $f$  value measurements are needed for the Ni I lines.

The Ni I line is assumed to contribute  $W_\lambda = 0.2$  mÅ to the 6363 Å line.

The 5577 Å line is blended with a C<sub>2</sub> doublet. The predicted C<sub>2</sub> contribution amounts to about 60 per cent of the observed 4 mÅ line. At present, this C<sub>2</sub> blend cannot be calculated with sufficient accuracy to enable the [O I] residual to be reliably estimated, i.e. a change of the C<sub>2</sub> contribution from 60 to 80 per cent is equivalent to a cut of the [O I] by a factor of 2. Therefore, the 5577 Å line is dropped from the list of O abundance indicators. Discussion of the [O I] transition probability was included to highlight the excellent experimental confirmation of the  $A$  value for this electric quadrupole transition. A reasonable inference is that the theoretical calculations of the similar [C I] line at 8727 Å are reliable.

## 2.4 ELECTRONIC TRANSITIONS OF THE CH RADICAL

### 2.4.1 CH in the Sun

The CH radical contributes to the Fraunhofer spectrum through the three electronic transitions  $A^2\Delta-X^2\Pi$ ,  $B^2\Sigma^- - X^2\Pi$  and  $C^2\Sigma^+ - X^2\Pi$ . The  $A-X$  system provides many lines from the  $\Delta v = 0$  sequence of bands near 4200 Å. Weaker  $\Delta v = -1$  bands near 4900 Å can also be identified but the lack of a reliable  $f$  value precludes their use as an abundance indicator. The  $B-X$  system (0, 0) and (1, 1) bands are near 3900–4000 Å with the weak (1, 0) band near 3650 Å also providing solar absorption lines. The  $C-X$  system is in a difficult spectral region [ $\lambda(0, 0) \sim 3140$  Å].

The dissociation energy of CH is known. Herzberg & Johns (1969) obtained  $D_0^0 = 3.454 \pm 0.012$  eV from the breaking off of emission in the  $B-X$  system. Recently, Brzozowski *et al.* (1976) have given an improved value,  $D_0^0 = 3.464 \pm 0.012$  eV, from an accurate study of the lifetimes of rotational levels in the  $B^2\Sigma^-$  state.

### 2.4.2 The $A-X$ system

Re-analysis of the CH  $A-X$  system is based on the equivalent widths listed by Grevesse & Sauval (1973, hereafter GS) who had access to the high signal-to-noise and high-resolution tracings that form the new Liège Atlas.

The  $f$  values for the (0, 0) and (1, 1) bands are calculated from the accurate radiative lifetimes (Brzozowski *et al.* 1976) obtained with the High Frequency Deflection technique (Erman 1975). The adopted results,  $f(0, 0) = 4.93 \times 10^{-3}$  and  $f(1, 1) = 4.88 \times 10^{-3}$ , are accurate to a few per cent.

### 2.4.3 The $B-X$ system

Rediscovery of the  $B-X$  system draws on the equivalent widths listed by GS. Although the  $f$  values for the  $B-X$  system are not quite so accurate as the  $A-X$  system values, an analysis is of value as it provides a check on possible wavelength-dependent errors.

The  $f$  values are obtained from a combination of radiative lifetime measurements (Brzozowski *et al.* 1976; see also Brooks & Smith (1974) and Anderson, Peacher & Wilcox (1975)) and *ab initio* calculations (Hinze, Lie & Liu 1975):  $f(0, 0) = 3.3 \times 10^{-3}$ ,  $f(1, 1) =$

$1.3 \times 10^{-3}$  and  $f(1, 0) = 1.2 \times 10^{-3}$ . Their accuracy should be about 10 per cent. The  $f$  value for an individual line includes a vibration–rotation factor estimate from Hinze *et al.*

A check on the  $f$  value for the (0, 0) band is provided by Linevsky's (1967) measurement of the relative  $f$  values of the  $A-X$  and  $B-X$  system. This study of the absorption lines produced by hot CH in a furnace gave  $f_{B-X}(0, 0)/f_{A-X}(0, 0) = 0.61 \pm 0.09$ . The adopted  $f$  values including the vibration–rotation factors give a ratio of 0.60 (the band  $f$  values give 0.67). The agreement is very pleasing.

#### 2.4.4 The C–X system

The  $C^2\Sigma^+ - X^2\Pi$  system [ $\lambda(0, 0) \sim 3140 \text{ \AA}$ ] is in a difficult spectral region and its contribution to the C abundance analysis is limited. Mount & Linsky (1974) analysed photoelectric tracings of the strong (0, 0) bandhead. Here, the bandhead is avoided and individual lines are selected. With the Moore & Broida (1959) identifications as a guideline, a list of about 30 apparently unblended CH lines was drawn up. Equivalent widths were taken from Moore, Minnaert & Houtgast (1966).

The lifetime of the  $C^2\Sigma^+$  state is very short and determined by a competing predissociation. The absorption  $f$  value can be deduced from the relative  $f$  values measured by Linevsky (1967). He gave the ratio  $f(C-X)/f(B-X) = 2.0 \pm 0.1$ . Correcting for the predicted rotational dependence of the  $f$  value, a band  $f$  value  $f(0, 0) = 5.8 \times 10^{-3}$  is obtained from  $f_{B-X}(0, 0) = 3.3 \times 10^{-3}$ . Linevsky also measured the ratio  $f(A-X)/f(B-X)$  and this together with the adopted  $f$  values gives  $f_{C-X}(0, 0) = 6.0 \times 10^{-3}$ . The *ab initio* calculations (Hinze *et al.* 1975) predict  $f_{C-X}(0, 0) = 7.95 \times 10^{-3}$ . The value  $f_{C-X}(0, 0) = 5.9 \times 10^{-3}$  is adopted. The uncertainty is perhaps  $\pm 15$  per cent. The vibration–rotation interaction factors are estimated from Hinze *et al.* (1975).

## 2.5 THE CN VIOLET AND RED SYSTEMS

### 2.5.1 CN in the Sun and stars

In late-type giants, the CN red system provides many weak and unblended lines from which the N abundance may be extracted given an independent determination of the C abundance. In these stars, CN is essentially the *only* monitor of the N abundance; the N I lines are too weak, the NH  $A-X$  system is located in the crowded ultraviolet spectrum and the NH vibration–rotation bands are undetectable. A critical analysis of the CN solar lines is a necessary step in the use of CN stellar lines.

At present, published values for the CN dissociation energy of seemingly similar reliability range from  $D_0^0 = 7.9$  to  $7.5 \text{ eV}$ ; the extreme range converts to a factor of 3 uncertainty in the C and N abundance product. What value should be adopted? The inquisitive astrophysicist is baffled by the variety of techniques employed and the substantial disagreements that remain. Gaydon (1968) reviewed the evidence, recommended  $D_0^0 = 7.75 \pm 0.2 \text{ eV}$  and commented 'it seems that many published estimates of limits of accuracy are optimistic'. Several new results were available to the compilers of the JANAF tables (Stull & Prophet 1971), who adopt a median value  $D_0^0 = 7.76 \pm 0.10 \text{ eV}$  with the comment that 'considerable scatter still exists and several sources of error are probable'. New  $D_0^0$  measurements to be taken into account are provided by Arnold & Nicholls (1973) and Engelman & Rouse (1975). Their methods are similar but the techniques (and results!) are different. Arnold & Nicholls observed CN emission from a shock tube and made a simultaneous determination of the CN dissociation energy and the absorption value of the violet system. Their  $f$  value is in excellent

agreement with the radiative lifetime measurements (see below). The dissociation energy obtained was  $D_0^0 = 7.89 \pm 0.13$  eV.

Recently, Engleman & Rouse (1975) reported a quantitative study of the absorption lines provided by hot CN molecules. CN was produced in a furnace at 1421 K and assumed to be in thermodynamic equilibrium with cyanogen ( $C_2N_2$ ) gas. Adopting the violet system  $f$  value deduced from the accurate lifetime measurement by Jackson (1974), they required  $D_0^0(\text{CN}) = 7.66 \pm 0.05$  eV to fit their absorption lines.

These two most recent determinations are in disagreement and underscore the JANAF comment that 'considerable scatter still exists'. Calculations reported here are based on the Engleman & Rouse value  $D_0^0 = 7.66$  eV. CN is *not* accepted as an abundance indicator because the  $D_0$  discrepancies are unresolvable at the present time. However, the Engleman & Rouse experiment is of appealing simplicity and a final value near 7.6 eV is likely.

### 2.5.3 The violet system

The  $B^2\Sigma^+ - X^2\Sigma^+$  violet system is a prominent contributor of Fraunhofer lines. The line selection is taken from GS and comprises weak to medium strong  $R$  branch doublets from the (0, 0) and (1, 1) bands. The  $\Delta v = -1$  sequence near 4200 Å is a potential source of weak lines. Earlier analyses of this sequence (Lambert, Hinkle & Mallia 1973; Grevesse & Sauval 1973) showed that the solar lines had equivalent widths about a factor of 2 larger than the predictions normalized to the (0, 0) band observations. This potential discrepancy prompted a thorough search of the new Liège Atlas with the initial aim being confirmation of the  $\Delta v = -1$  identifications. A positive identification was established. Equivalent widths were measured for CN lines on blends.

The oscillator strengths for the  $B-X$  system may be derived from the accurate measurement of the radiative lifetime of the  $B^2\Sigma^+$  state (Jackson 1974, and references therein). A tunable dye laser was used to excite CN molecules. The lifetime  $\tau = 65.6 \pm 1.0$  ns for the  $v = 0$  vibrational level corresponds to an electronic  $f$  value  $f = 0.0342 \pm 0.0005$ . This assumes that the radiative lifetime is dominated by the contribution from the  $B-X$  system. The competing  $B-A$  system is obviously weak but an accurate branching ratio is unavailable; Liszt & Hesser (1970) estimate that the  $B-A$  contribution to the lifetime does not exceed 5 per cent.

The radiative lifetime of the  $B^2\Sigma^+$  state is controlled by the  $\Delta v = 0$  sequence.  $f$  values for the weak off-diagonal bands are calculated using the Franck-Condon factors obtained from RKR potential calculations and the transition moment variation with internuclear separation consistent with the lifetime measurements by Liszt & Hesser (1970) and the emission line analysis by Arnold & Nicholls (1973). The  $f$  values for the bands used in this solar abundance analysis are

$$\begin{array}{ll} f(0, 0) = 0.0342 & f(0, 1) = 0.00240 \\ f(1, 1) = 0.0268 & f(1, 2) = 0.00425 \\ f(2, 2) = 0.0229 & f(2, 3) = 0.00515. \end{array}$$

The  $\Delta v = 0$   $f$  values should be accurate to 5 per cent or better. The weaker  $\Delta v = -1$   $f$  values are less accurate.

### 2.5.4 The red system

The  $A^2\Pi - X^2\Sigma^+$  red system with a (0, 0) band near 1.1 micron and many weaker bands is an apparently attractive candidate for inclusion in an abundance analysis. This analysis adopts

the GS line list for the (0, 0) band. Unfortunately, the  $f$  values for the system are poorly determined – see reviews by Grevesse & Sauval (1973) and Arnold & Nicholls (1972).

Arnold & Nicholls (1972) analysed the CN emission produced by a shock tube experiment and obtained  $f(0, 0) = (2.2 \pm 0.4) \times 10^{-3}$  for an assumed dissociation energy  $D_0^0 = 7.89$  eV. Treffers (1975) obtained  $f(0, 0) = (3.3 \pm 0.7) \times 10^{-3}$  ( $D_0^0 = 7.66$  eV assumed) through an analysis of CN emission from a furnace. If a lower  $D_0^0$  were preferred, these  $f$  values would be increased. Analysis of the solar (0, 0) lines suggests a rather lower  $f$  value, i.e.  $f(0, 0) \sim 1.6 \times 10^{-3}$  for  $D_0^0 = 7.89$  eV (see Section 4.5).

In view of the lack of a definitive lifetime measurement (i.e. an application of the High Frequency Deflection technique) and the disagreement between the observed and predicted equivalent widths, a recommended  $f$  value is not presented.

## 2.6 ELECTRON TRANSITIONS OF C<sub>2</sub>

### 2.6.1 The Swan system

The C<sub>2</sub> Swan bands contribute numerous weak lines to the solar spectrum. In the revised notation (Herzberg, Lagerqvist & Malmberg 1969), this is the  $d^3\Pi_g - a^3\Pi_u$  transition. Equivalent widths for (0, 0) lines between 4916 and 5164 Å were tabulated by GS. Independent measurements for (0, 0) and (1, 1) lines were kindly provided by Dr E. A. Mallia (private communication) from photoelectric tracings obtained at the Gornegrat outstation of the Department of Astrophysics in Oxford (Blackwell, Mallia & Petford 1969). These spectra are slightly inferior in resolution but have a similar signal-to-noise ratio as those available to GS. In Fig. 1, an equivalent width comparison is shown for lines common to the two lists. The small scatter reflects inevitable differences in continuum placement and in the correction for very weak blends. Clearly, the equivalent width accuracy for these weak lines is now quite satisfactory for abundance purposes. The solar observations (Lambert & Mallia 1974) of the C<sub>2</sub> Phillips system are too uncertain for inclusion in an abundance analysis.

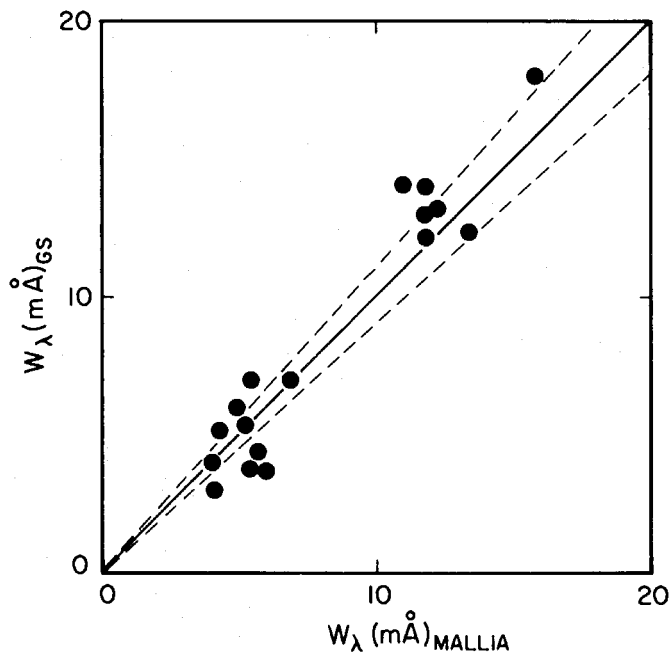


Figure 1. Comparison of the equivalent widths ( $W_\lambda$ ) for C<sub>2</sub> Swan band lines as measured by Grevesse & Sauval (1973) and Mallia (private communication). The solid line has unit slope with the broken lines indicating the 10 per cent error limits.

### 2.6.2 The $C_2$ dissociation energy

The dissociation energy appears to be well determined thanks to the spectroscopic detective work by Messerle & Krauss (1967a). Predissociation by rotation was observed and a well defined limiting curve gave  $D_0^0 = 6.11 \pm 0.04$  eV. The dissociation products were unambiguously determined.

Messerle & Krauss (1967b) also undertook an extrapolation of the vibrational levels of  $d^3\Pi_g$  and  $e^3\Pi_g$  state using a new extrapolation formula to obtain  $D_0^0 = 6.07$  and  $6.09$  eV respectively. However, as Herzberg *et al.* (1969) point out, the validity of the formula has not been checked.

This and other non-spectroscopic results are consistent with  $D_0^0 = 6.11 \pm 0.04$  eV and this value is adopted (see Gaydon 1968).

### 2.6.3 Swan system $f$ value

The  $f$  value for the Swan bands has been measured by a variety of techniques. No theoretical calculations achieve an accuracy comparable with that of the best experiments. A recent and extensive programme of radiative lifetime measurements for the  $d^3\Pi_g$  upper state was reported by Curtis, Engman & Erman (1976) using the High Frequency Deflection technique. Lifetimes for vibrational levels  $v = 0$  to  $v = 6$  were measured with a precision of about 5 per cent using narrow spectral regions around the bandheads and, also, some individual rotational triplets. Their lifetimes  $\tau(v = 0) = 123 \pm 6$  ns and  $\tau(v = 1) = 124 \pm 6$  ns provide  $f$  values:  $f(0, 0) = 0.0239 \pm 0.0012$  and  $f(1, 1) = 0.0108 \pm 0.0006$  when the variation of the electronic transition moment with internuclear separation given by Danylewych & Nicholls (1974) is adopted. On the reasonable assumption that the measured lifetimes are unaffected by a competing predissociation process, the variation of the measurements with the vibrational level can be shown to be in excellent accord with the predictions based upon the transition moment variation derived from band intensities; e.g. Danylewych & Nicholls (1974, Table 5) predict a ratio  $\tau(v = 4)/\tau(v = 0) = 1.11$  and Curtis *et al.* report  $\tau(v = 4) = 131 \pm 6$  ns and  $\tau(v = 0) = 123 \pm 6$  ns or  $\tau(v = 4)/(v = 0) = 1.07$ . The above  $f$  values are adopted.

Several independent shock tube  $f$  value measurements are available in which the  $C_2$  Swan band was observed either in absorption or in emission (see Cooper & Nicholls 1975, for references). The results (uncertainties of 15–30 per cent) fall in the range  $0.016 \leq f(0, 0) \leq 0.025$ . Danylewych & Nicholls (1974) suggest a ‘best’ value of  $f(0, 0) = 0.021$ . This is slightly smaller than our adopted lifetime result but well within the combined uncertainties. In part, the discrepancy is attributable to the higher dissociation energy ( $D_0^0 = 6.25$  eV) adopted in most thermochemical calculations. If the lower and preferred value ( $D_0^0 = 6.11$  eV) were adopted, the shock tube  $f$  values would have to be increased and the small discrepancy with the lifetime measurement would be reduced. Danylewych & Nicholls also provide references to other  $f$  value measurements that are not competitive with either the lifetime or shock-time experiments.

## 2.7 THE NH RADICAL

### 2.7.1 The $A-X$ system

Strong absorption features attributable to compact  $Q$  branches of the  $A^3\Pi-X^3\Sigma^-$  transition are unmistakable signatures of the imidyl (NH) radical. Although the NH lines are in the ultraviolet, this molecule provides a useful cross-check on the N abundance. Other electronic transitions in NH are known but none can be identified in the photospheric spectrum.

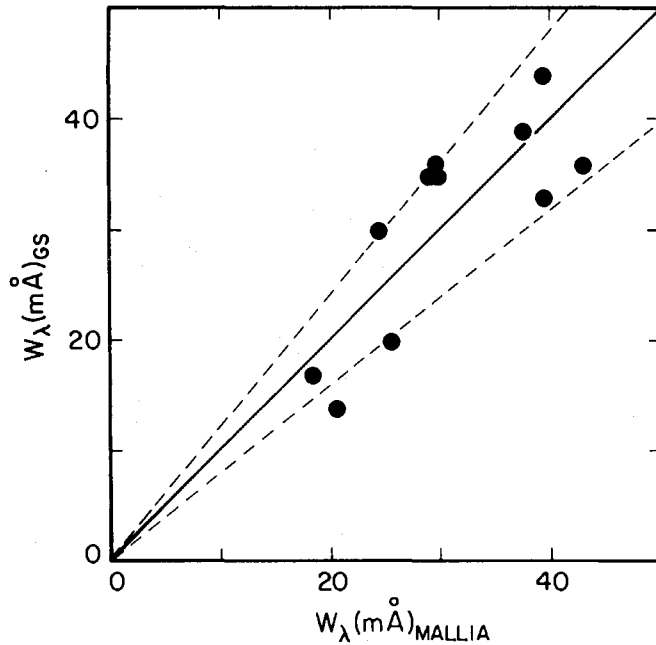


Figure 2. Comparison of the equivalent widths for NH  $A-X$  system lines as measured by Grevesse & Sauval (1973) and Mallia (private communication). The solid line has unit slope. Broken lines indicate the 10 per cent error limits.

The analysis uses equivalent widths kindly provided by Dr E. A. Mallia from photoelectric tracings. Comparison (Fig. 2) for common lines shows good agreement with the measurements by GS.

### 2.7.2 The NH dissociation energy

New spectroscopic evidence has injected apparent confusion into the NH dissociation energy discussion. Before the appearance of this evidence, the compilers of the JANAF tables (Chase *et al.* 1974) recommended  $D_0^0 = 3.21 \pm 0.2$  eV and remarked ‘the reason for the choice is that it is consistent with *all* the experimental data’. Primary evidence for this value comes from Seal & Gaydon’s (1966) shock tube study of NH absorption lines. The variation with temperature of the NH column density (obtainable via the  $f$  value for the  $A-X$  system) at known pressures yielded the dissociation energy:  $D_0^0 = 3.21 \pm 0.16$  eV. Their adopted  $f$  value does not differ significantly from the current best value. Confirmation of the  $D_0^0$  value was provided by Kaskan & Nadler (1972) using a  $\text{NH}_3/\text{O}_2/\text{N}_2$  flame. Their determination of the heat of formation of NH converts to  $D_0^0 = 3.17 \pm 0.22$  eV (see Stevens 1973). This value was not included by the JANAF compilers (Chase *et al.* 1974).

Electron impact experiments (Reed & Snedden 1958; Franklin *et al.* 1958) have given higher  $D_0^0$  values ( $D_0 \sim 3.5$  eV). Gaydon (1968) suggested that these experiments be considered as providing an upper limit to  $D_0^0$  because electron impact studies often involve excess energy. Kaskan & Nadler also give reasons for preferring a lower value for  $D_0^0$ . None the less, the discrepancy is disquieting.

New spectroscopic evidence does not still the disquiet. Masanet, Gilles & Vermeil (1974) have discovered the intercombination  $b^1\Sigma^+ - X^3\Sigma^-$  transition which leads to an accurate determination of the singlet–triplet splitting:  $T_0(a^1\Delta) - T_0(X^3\Sigma^-) = 1.561$  eV. Observations of diffuse emission lines in the  $d^1\Sigma^+ - c^1\Pi$  system led Krishnamurty & Narasimham (1969) to propose that rotational levels  $J \gtrsim 24$  in the lowest vibrational level of the  $c^1\Pi$  state were

subject to predissociation by rotation. Smith, Brzozowski & Erman (1976) use the predissociation observations to estimate the dissociation energy of the  $c^1\Pi$  state and combine this with the triplet–singlet splitting to obtain  $D_0^0 = 3.95$  eV for the  $X^3\Sigma^-$  ground state. This is clearly in conflict with the value  $D_0^0 = 3.2$  eV suggested by the JANAF compilers. The uncertainty assigned by Smith *et al.* is  $\pm 0.07$  eV and, although the predissociation observation can establish only an upper limit to the  $D_0^0$  value for the  $c^1\Pi$  state, the correction is probably small ( $\leq 0.1$  eV). Resolution of the conflict is impossible at this time; it appears that either the earlier experiments are seriously in error or the diffuse emission lines are incorrectly attributed to predissociation by rotation. Additional spectroscopic observations are urgently needed.

Several theoretical calculations are relevant to the  $D_0^0$  problem. An *ab initio* calculation by the method of optimized valence configurations was reported by Stevens (1973):  $D_0^0 = 3.18 \pm 0.2$  eV. The uncertainty is assessed from predictions by the same method for OH and HF for which reliable experimental results are available. Another *ab initio* calculation (Liu & Verhaegen 1971) using the LCAE-MO-SCF method yields  $D_0^0 = 3.31$  with a probable uncertainty of 0.1 eV (Verhaegen 1972, private communication).

These two calculations do not support the high  $D_0^0$  value derived from the predissociation argument. A third calculation produces an accurate  $D_0^0$  value. Meyer & Rosmus (1975) employ variational configuration interaction wavefunctions and the coupled electron-pair approximation to predict a variety of molecular properties including  $D_0^0$ . A correlation contribution to  $D_0^0$  is derived empirically by comparing predicted and observed  $D_0^0$  values for OH and HF. Then, they recommend a value  $D_0^0 = 3.40 \pm 0.05$  eV. Their recommendation is adopted. It is consistent with all the experimental work and conflicts only with the new spectroscopic estimate. A pertinent remark to add is that their recommendation for MgH,  $D_0^0 = 1.23 \pm 0.05$  eV is confirmed by recent spectroscopic analysis (Balfour & Cartwright 1975, 1976).

### 2.7.3 *f* values for the *A*–*X* system

A detailed study for the  $A^3\Pi$  state by Smith, Brzozowski & Erman (1976) is based on the High Frequency Deflection technique and lifetime measurements with an accuracy of about 1 per cent at a spectral resolution of 0.06 Å. For  $N \geq 24$  in  $v = 0$  and  $N > 13$  in  $v = 1$ , the lifetimes are reduced by predissociation. Lifetimes of states unaffected by predissociation show a slight increase with increasing rotation (e.g.  $\tau = 404 \pm 5$  ns ( $N = 4$ ) to  $451 \pm 4$  ns ( $N = 23$ ) for  $v' = 0$  and  $\tau = 413 \pm 6$  ns ( $N = 5$ ) to  $424 \pm 6$  ns ( $N = 14$ ) for  $v = 1$ ) which is attributable to a decrease of the electronic transition moment with increasing internuclear separation. Since the effect is of the same order or less than errors in the equivalent width estimates, a mean value is adopted and the vibration–rotation interaction is ignored:  $\tau(v = 0) = 410$  ns and  $\tau(v = 1) = 420$  ns yield  $f(0, 0) = 8.24 \times 10^{-3}$  and  $f(1, 1) = 8.09 \times 10^{-3}$ .

Earlier lifetime results, which lacked the precision and spectral resolution attainable with the High Frequency Deflection technique, are referenced by Grevesse & Sauval (1973).

## 2.8 THE OH RADICAL

### 2.8.1 The *A*–*X* system

Unknown continuous or quasi-continuous opacity sources affect the solar ultraviolet spectrum. The OH  $A^2\Sigma^+ - X^2\Pi$  system should provide a useful measure of their effect on the molecular lines; the OH dissociation energy and the *f* value of the *A*–*X* system are known.

Equivalent widths of OH (0, 0) band lines are taken from GS. The dissociation energy  $D_0^0 = 4.391 \pm 0.002$  eV (Carlone & Dalby 1969) is adopted.

### 2.8.2 $f$ values for the $A-X$ system

Numerous measurements are reported in the literature for the radiative lifetime of the  $a^2\Sigma^+$  state. Applications of pulsed dye lasers are providing new results. German (1975a, b) excites OH in a very low pressure flow cell ( $p < 1$  mtorr) and obtains a mean value  $\tau = 690 \pm 20$  ns for the rotationless molecule in the ground vibrational level. Other experiments at higher gas pressures show a rather wide dispersion in the reported lifetimes:  $\tau = 820 \pm 40$  ns (Becker, Haaks & Tatarczyk 1974),  $788 \pm 13$  ns (Brophy, Silver & Kinsey 1974) and  $720 \pm 30$  ns (Hogan & Davis 1974). German has also studied the lifetime variation up the rotational ladder and in the excited vibrational levels  $v = 1$  and 2.

Other lifetime measurements in which excited OH radicals are produced by dissociative excitation of water vapour are reported by Elmergreen & Smith (1972) and Sutherland & Anderson (1973). The radiative lifetime for the rotationless molecule in the  $v = 0$  state is about  $740 \pm 30$  and  $755 \pm 20$  ns from these two experiments. Experiments utilizing the Hanle effect are reviewed by German (1975a) and, presently, they appear not to provide data of sufficient quality to resolve the above lifetime discrepancies. Other  $f$  value measurements based upon absorption or emission line intensities are not competitive with the lifetime measurement accuracy; references can be traced through GS.

The adopted lifetime is  $\tau = 700$  ns for the rotationless molecule in the  $v = 0$  level, i.e. greatest weight is assigned to the laser fluorescence experiment by German (1975a). The equivalent  $f$  value is  $f(0, 0) = 9.4 \times 10^{-4}$ . The uncertainty is not in excess of 10 per cent.

Vibration-rotation interaction is significant within the  $A-X$  system. A calculation by Anketell & Learner (1967) is adopted; they find the interaction reduces the  $f$  values by about 40 per cent out to  $J \sim 25.5$  along the rotational ladder. A more recent discussion (Crosley & Lengel 1975) suggests that some revision of these results may be necessary.

## 2.9 THE CO VIBRATION-ROTATION BANDS

The CO molecule satisfies some important requirements for the ideal abundance indicator; the dissociation energy is well determined ( $D_0^0 = 11.091 \pm 0.019$  eV, see reviews by Brewer & Searcy (1956) and Gaydon (1968), a rich supply of lines is available in the fundamental and first-overtone vibration-rotation bands of the  $X^1\Sigma^+$  ground state for which reliable  $f$  values are available. The ultraviolet  $A-X$  (Fourth Positive System) transition is dismissed on account of the extreme line crowding and uncertainty over the continuous opacity contributors. Unfortunately, the stated advantages of CO are partially offset by the large dissociation energy and the resultant sensitivity of the abundance results to the photospheric temperature profile.

The CO equivalent widths are measured from the Hall (1972) infrared atlas. Newkirk's (1957) line list was used. The new  $W_\lambda$ 's are about 10 per cent larger than Newkirk's values.

The  $f$  values are calculated from Tipping's (1976) recipe which represents a synthesis of the best of the available experiments. The new  $f$  values differ by less than 10 per cent from the Young & Eachus (1966) results adopted in the 1968 analysis.

## 3 Model solar atmospheres

Five model atmospheres were culled from the recent literature. They were taken from the following references: Holweger & Müller (1974 – see also Holweger 1967), Gingerich *et al.*

(1971 – this is the Harvard–Smithsonian reference atmosphere), Vernazza, Avrett & Loeser (1976), Ayres & Linsky (1976) and Allen (1976, in preparation). They will be identified in the following discussion as models HM, HSRA, VAL, AL and A. All five are empirical atmospheres based in part on observations of the continuous spectrum.

A partial assessment of the five models is presented here. The first test utilizes the measurements of the absolute intensity at the centre of the solar disk reported by Labs & Neckel (1968, 1970, 1971, 1972), Labs (1975) and Neckel (1975) for the wavelength interval  $5000 \text{ \AA} \leq \lambda \leq 12\,500 \text{ \AA}$ . Below  $5000 \text{ \AA}$ , present knowledge of the (effective) continuous absorption coefficient is sufficiently incomplete to invalidate a comparison of model atmosphere predictions with the observations. Between  $12\,500 < \lambda < 25\,000 \text{ \AA}$ , the primary information comes by fitting relative intensity measurements by Pierce (1954) to the long wavelength end of the Labs & Neckel observations. Unfortunately, the fit is not unique and the resultant uncertainty is large relative to the difference in the predictions from the five models. The Labs & Neckel observations would appear to be superior to more recent measurements made from high-altitude aircraft (see comments by Neckel 1975; also Lambert 1971). In Fig. 3, a comparison is presented between the observed and predicted brightness temperatures. Within the 2 per cent uncertainty of the observations, models H and A reproduce the observations satisfactorily, models VAL and HSRA are marginally inconsistent and model AL can be rejected through this comparison. Clearly, the comparison is a test of the deep layers in which the high excitation C I, N I and O I lines are formed. This test sheds little light on the accuracy of the models in the region of molecular line formation.

Limb darkening observations in the interval  $0.5 < \lambda < 2.5 \mu\text{m}$  provide a test of the models over a greater optical depth range. In Fig. 4, observations and predictions are compared for disk positions  $\cos \theta = 0.2$  and  $0.4$  ( $\theta$  is the angle between the line of sight and the normal to the surface). At  $\cos \theta = 0.2$ , the minimum brightness temperature is near  $5250 \text{ K}$  so that the continuum radiation encroaches upon the molecular line forming region. The observations

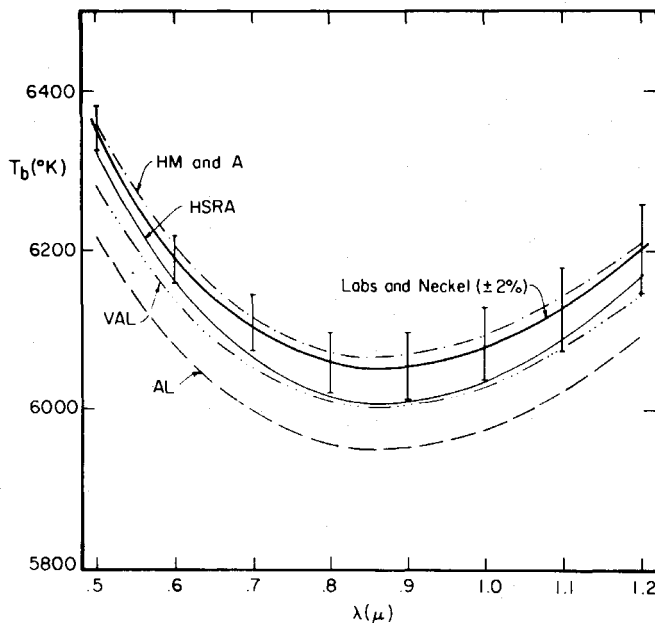


**Figure 3.** Variation of solar (centre of disk) brightness temperature with wavelength. The thick solid line (and 2 per cent error bars) shows the observed brightness temperature according to Labs & Neckel. Predictions from the five model atmospheres are indicated; the models HM and A give almost identical predictions and a single curve is shown for these models.

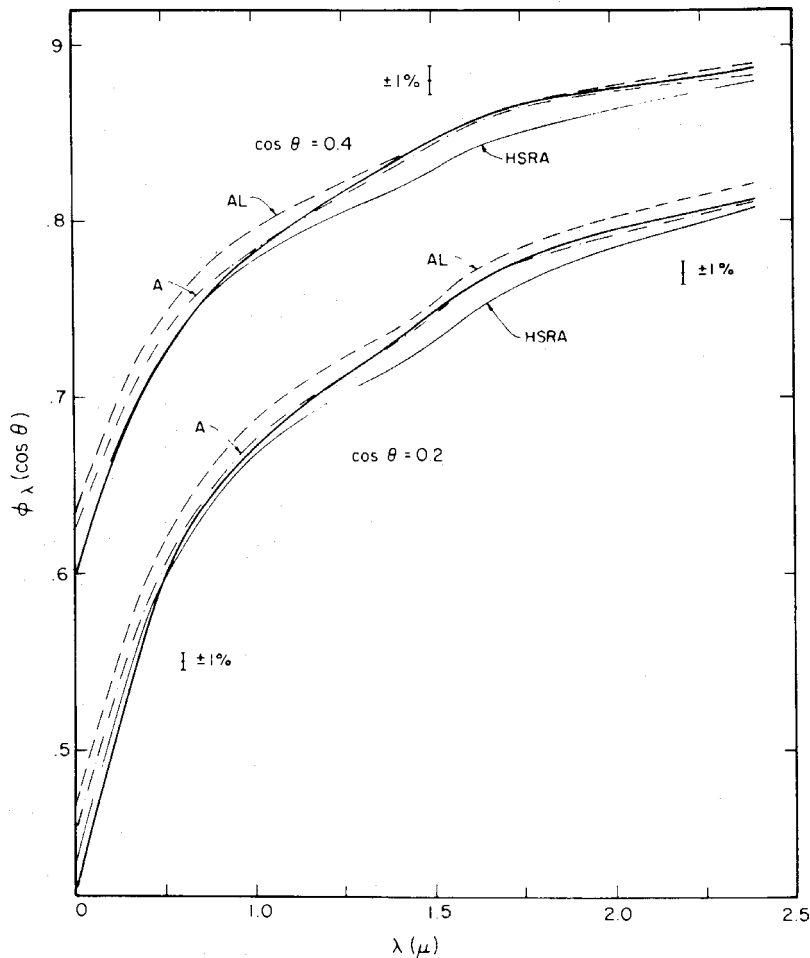


**Figure 4.** Limb-darkening observations,  $\phi_\lambda(\cos\theta) = I_\lambda(\cos\theta)/I_\lambda(1.0)$  where  $I_\lambda$  is the emergent specific intensity, for the disk positions  $\cos\theta = 0.2$  and  $0.4$  and the wavelength interval  $0.5\text{--}2.4\ \mu\text{m}$ . The observations are represented by the thick solid line. Predictions for the three models AL, A and HSRA are identified. The model HM gives predictions that are almost coincident with those for model A.

are taken from Lambert (1965, 1971). For  $1 < \lambda < 2.5\ \mu\text{m}$ , the observations are a mean of separate and concordant investigations by Pierce (1954 – as corrected by David & Elste 1962) and Lambert (1965); observational uncertainty is about 1 per cent. Shortward of  $1\ \mu\text{m}$ , David & Elste's tabulation is used to derive the interpolated curves.

Models A (and HM) fit the observations very closely for  $\lambda \geq 0.9\ \mu\text{m}$ ; model A is based on new unpublished limb-darkening observations so that the agreement with the older observations suggests that the latter are free from significant systematic errors. For  $\lambda < 0.9\ \mu\text{m}$ , the model A (and HM) predictions diverge from the observations as found earlier (Lambert 1965, 1971) in an attempt to construct a model with the maximum agreement with continuum observations. The source of this discrepancy is unidentified but probable causes (additional opacity from weak, unidentified and overlapping absorption lines, non-linearity in averaging over the solar granulation, an error in the short-wavelength observations) are linked to the short wavelengths so that the better models should be those which fit the long-wavelength ( $\lambda > 0.9\ \mu\text{m}$ ) observations at the expense of a poor fit at shorter wavelengths. At the positions  $\cos\theta = 0.2$  and  $0.4$ , models HSRA and AL show predicted intensities that are not consistent with the observations. Model VAL (predictions are not plotted in Fig. 4) must be ruled acceptable but the fit to the observations is inferior to that provided by models HM and A.

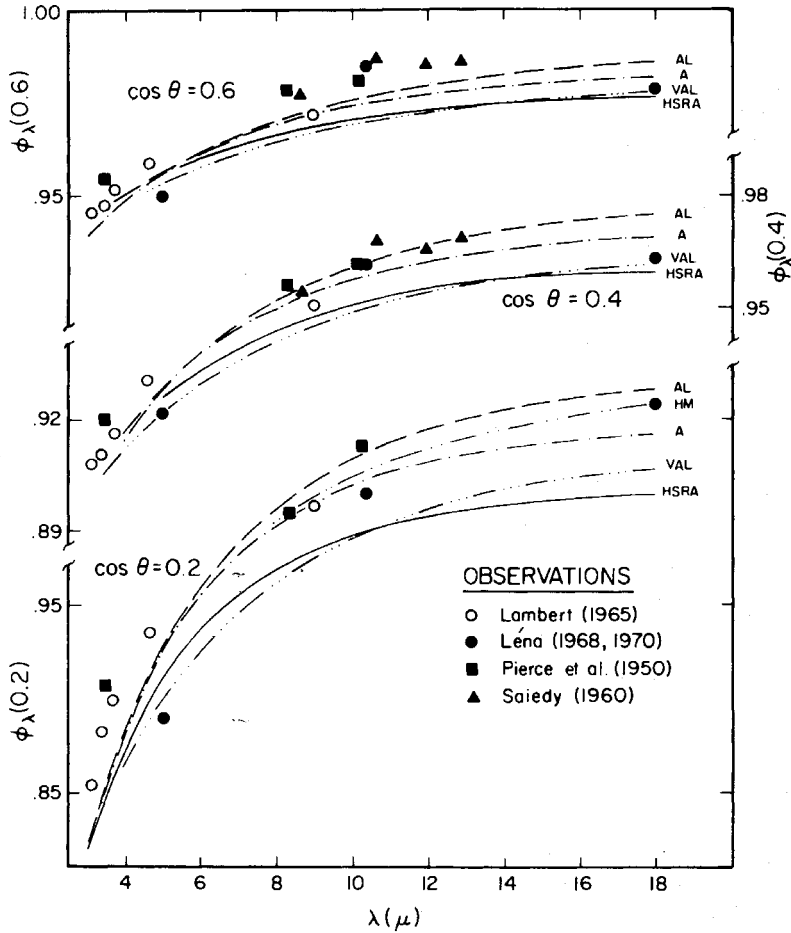


**Figure 5.** Limb darkening observations,  $\phi_\lambda(\cos \theta)$ , for disk positions  $\cos \theta = 0.2, 0.4$  and  $0.6$  and the wavelength interval  $3\text{--}18\ \mu\text{m}$ . Observations are identified in the key. Model predictions are shown. At  $\cos \theta = 0.4$  and  $0.6$ , predictions for model HM are not displayed; they are very close to those for model A.

The  $\text{H}^-$  free–free opacity increases as the square of the wavelength and, therefore, a comparison of the observed and predicted continuum radiation for  $\lambda > 2.5\ \mu\text{m}$  constitutes a test of the temperature–optical depth function for higher photospheric layers including the molecular line-forming region. Examination of the model predictions for the absolute intensity at the centre of the solar disk to  $20\ \mu\text{m}$  show that none of the present five can be rejected; the observational uncertainty prohibits a discrimination between the five models. Vernazza, Avrett & Loeser (1976) present a summary of the available measurements.

Limb-darkening observations for the  $3\text{--}18\text{-}\mu\text{m}$  interval are available – see Fig. 5 for the references. The predictions for  $\cos \theta = 0.2$  and  $0.4$  show that models HSRA and VAL are probably in conflict with the observations. The three models HM, A and AL provide an adequate fit to the limited observations. Léna’s (1970)  $5\text{-}\mu\text{m}$  limb-darkening observations maybe affected by CO lines within the bandpass. The observations (Pierce *et al.* 1950; Lambert 1965) for the  $3\text{--}5\ \mu\text{m}$  window show a systematic departure from all the predictions; new observations are needed to eliminate the possibility of a systematic error affecting the observations. The brightness temperature at  $18\ \mu\text{m}$  and  $\cos \theta = 0.2$  is near  $4700\ \text{K}$  so that Fig. 5 does represent a test of the temperature profile within the molecular line forming regions; estimates of the rotational temperatures for the  $\text{C}_2$  Swan and CN red system lines range from about  $T = 5000$  to  $4700\ \text{K}$ . The opacity increase in the ultraviolet can also be used to test the upper photospheric layers of the models. Unfortunately, the

observational accuracy and the lack of a detailed accounting for all the absorption lines are severely limiting factors.

These comparisons between the predicted and observed continuous spectrum suggest the following ranking for the five selected models. Models HM and A provide a good fit to the observed spectrum. Model VAL is marginally deficient. Models AL and HSRA can be rejected because they fail to fit the observations.

All five models ignore the solar granulation with the implicit assumption that the homogeneous or one-stream model derived from spatially averaged observations (usually of the continuum) is applicable to all absorption lines. Even cursory inspection shows that the assumption is of doubtful validity when applied across the extreme range represented by the CO and permitted C I, N I and O I lines included in this study. A preliminary assessment of the effects of granulation has been attempted using an inhomogeneous or two-stream model. The temperature difference between the hot and cold streams was about 900 K for  $\tau_0 < 0.4$  and decreased smoothly to zero at  $\tau_0 \sim 4$ . Hydrostatic equilibrium was assumed for each stream. The composite spectrum is calculated by giving equal weight to the two streams. The abundances are compared with those obtained from a model with a mean temperature profile.

The photospheric velocity field is a component of the model atmosphere. The critical item in an abundance analysis is the microturbulent velocity field. Microturbulence, by definition, is the component of the velocity field which affects the saturation of a line. Here, the effect of the microturbulence is minimized by using weak lines. All calculations were undertaken with a uniform microturbulence of  $\xi_{\text{mic}} = 1.0$  km/s.

Extraction of the microturbulence from a set of solar absorption lines requires accurate  $f$  values. Precision Fe I  $f$  values (maximum error  $\sim 0.02$  dex) and accurate equivalent widths are combined by Blackwell *et al.* (1976) who derive a microturbulence for the centre of the disk of  $\xi_{\text{mic}} = 0.8$  km/s (model HSRA) and 0.9 km/s (model HM). These authors also list recent determinations of the microturbulence spanning the range 0–3.4 km/s. The adopted value,  $\xi_{\text{mic}} = 1.0$  km/s, was selected prior to Blackwell *et al.* study and represents a rough average over the more accurate of recent studies. Holweger & Müller (1974) present a velocity field (micro plus macroturbulence) in which the vertical component of  $\xi_{\text{mic}}$ , which is of interest to this analysis of equivalent widths obtained at the centre of the disk, runs from  $\xi_{\text{mic}} = 0.5$  km/s at  $\tau_{0.5} = 0.01$  to  $\xi_{\text{mic}} = 1.6$  km/s at  $\tau_{0.5} = 1.0$ . A depth dependence is ignored in the present calculations.

## 4 The abundance analysis

### 4.1 SELECTION OF MODEL ATMOSPHERES AND LINES

The entire list was subjected to analysis with the five model atmospheres and yielded the abundances listed in Tables 4, 5 and 6. The abundance is given as  $\log \epsilon$  on the standard scale  $\log \epsilon(\text{H}) = 12.00$ . The rms error ( $\sigma$ ) in these tables is calculated from the abundance spread of the lines. This error does not include the effects of external errors such as the uncertainty in the dissociation energy of a molecule.  $\sigma$  is tabulated for model HM, results are essentially identical for all models. The dependence of the abundances on the microturbulence is shown by  $\Delta_{\text{mic}}$  which gives (in dex) the abundance increase required as the microturbulence is cut from 1 km/s to 0.5/s.

A subset of the lines and model atmospheres can be recognized as the superior abundance indicators and includes: [C I]  $\lambda 8727$ , CH A–X, C<sub>2</sub> Swan, N I, [O I]  $\lambda\lambda 6300, 6363$ . Other species from Tables 3, 4 and 5 are relegated to a supporting role for a variety of reasons as discussed in preceding sections. Exclusion of the permitted C I and O I from the ‘superior’

Table 4. Carbon abundance summary.

Species	Holweger–Müller			Allen	Vernazza	HSRA	Ayres– Linsky
	log $\epsilon$	$\sigma$	$\Delta_{\text{mic}}$	log $\epsilon$	log $\epsilon$	log $\epsilon$	log $\epsilon$
[C I] $\lambda$ 8727	8.69	—	0.00	8.65	8.70	8.64	8.66
C I	8.56	0.11	0.02	8.52	8.62	8.53	8.64
CH $A-X$	8.67	0.07	0.02	8.57	8.60	8.49	8.61
$B-X$ (0, 0)	8.59	0.05	0.01	8.50	8.52	8.41	8.54
(1, 0)	8.65	0.10	0.01	8.54	8.56	8.47	8.57
(1, 1)	8.68	0.19	0.02	8.58	8.61	8.51	8.61
$C-X$ (0, 0)	8.77	0.22	0.02	8.69	8.68	8.58	8.70
C <sub>2</sub> Swan	8.73	0.04	0.00	8.69	8.69	8.64	8.70
CO 2.3 $\mu\text{m } V-R^*$	8.71	0.06	0.00	8.52	8.38	8.38	8.64

\* Derived using the O abundances given by the [O I] lines -- see Table 6.

Table 5. Nitrogen abundance summary.

Species	Holweger–Müller			Allen	Vernazza	HSRA	Ayres– Linsky
	log $\epsilon$	$\sigma$	$\Delta_{\text{mic}}$	log $\epsilon$	log $\epsilon$	log $\epsilon$	log $\epsilon$
NI	7.98	0.06	0.02	8.01	8.04	7.93	8.09
NH $A-X$	7.99	0.15	0.02	7.87	7.88	7.79	7.90
CN Violet*	7.85	0.05	0.02	7.81	7.75	7.75	7.84

\* Derived using the mean C abundances from Table 4.

category is based on the  $f$  value uncertainties and the possible effects of departures from local thermodynamic equilibrium. Similar remarks can probably be addressed to the NI lines. The CH  $B-X$  and  $C-X$  systems are inferior to the  $A-X$  systems in terms of the  $f$  values and the location of the  $B-X$  and  $C-X$  lines in the ultraviolet where line blending is more serious and present information on the continuous absorption coefficient is incomplete.

In Section 3, the restricted comparison with observations of the visible and infrared continuous spectrum suggested that models HSRA and AL gave an inadequate fit to the observations. The best fits were found from models HM and A. Model VAL was ruled to be acceptable. A conclusion is that models HM and A should be adopted for the final abundance derivations to which the other models contribute an estimate of the abundance errors attributable to the model atmosphere uncertainties.

#### 4.2 THE CARBON ABUNDANCE

The three superior C indicators show a consistent abundance when analysed with model HM. In 1968, attention was drawn to a discrepancy between the C abundance provided by the CH  $A-X$  lines and the other C indicators ([C I], C I and C<sub>2</sub>). Inspection of Table 4 shows that similar discrepancies exist for model HSRA and at a smaller level for other models. Perhaps, the resolution of this discrepancy is an additional point in favour of model HM.

Inclusion of the [C I] line is based on the assumption that this weak line is unblended. Lambert & Swings (1967a) noted a very weak Fe I line as a blend. In G and K giants, the [C I] lines may be blended with an unidentified line in addition to weak <sup>13</sup>CN and FeH

blends but it is unlikely that this line can contaminate the solar spectrum (Lambert & Ries 1977).

Although the inspection of Table 4 shows the C<sub>2</sub> Swan system to be less sensitive than the CH *A–X* system to the model atmosphere (this is attributable to the obvious fact that the C<sub>2</sub> lines depend on the square of the C abundance), C<sub>2</sub> and CH are given an equal weight because the C<sub>2</sub> dissociation energy is the more uncertain:  $\Delta D_0^0 \sim 0.04$  eV for C<sub>2</sub> to  $\sim 0.012$  for CH.

In deriving a mean C abundance, [C I], CH *A–X* and C<sub>2</sub> are assigned equal weight. Results are  $\log \epsilon(\text{C}) = 8.69$  (HM), 8.64 (A), 8.66 (VAL), 8.59 (HSRA) and 8.67 (AL). All supporting indicators are consistent with the above C abundances.

The interagreement between the several CH systems indicates that the lack of a complete accounting for the continuous opacity in the ultraviolet can have only a small effect on an abundance derived from a hydride. The CH *B–X* (0, 0) band is the most reliable of these additional systems and the derived abundance ( $\log \epsilon(\text{C}) = 8.59 \pm 0.05$ , model HM) is consistent with that from the *A–X* system ( $\log \epsilon(\text{C}) = 8.67 \pm 0.07$ , model HM).

The CO vibration–rotation 2.3  $\mu\text{m}$  lines are relegated to a supporting role on account of their model atmosphere sensitivity through the high dissociation energy. These lines monitor the product of the carbon and oxygen abundances. The C abundance attributed to the CO lines in Table 4 is derived using the mean O abundances from the [O I] lines for the individual models. The result for model HM is quite consistent with that from the best abundance indicators. Models VAL and HSRA show a significant discrepancy between CO and other indicators.

If models HM and A are assigned an equal weight, the mean abundance from the superior indicators is  $\log \epsilon(\text{C}) = 8.67$ . Examination of Table 4 and the review of sources of external error in the atomic and molecular indicators that the uncertainty is probably smaller than  $\pm 0.10$  dex. Possible errors arising from breakdown of LTE and the introduction of an inhomogeneous (two-stream) model are examined in the concluding section.

This new abundance is 0.12 dex higher than 1968 value. Throughout the discussion, no support has been found for the low C abundance ( $\log \epsilon(\text{C}) = 8.35 \pm 0.15$ ) proposed recently by Mount & Linsky (1975). In part, their low abundance rests heavily on the CN violet system for which they adopted a high dissociation energy ( $D_0^0 \sim 7.9$  eV) which may now be in doubt (see Section 2.5.2).

### 4.3 THE NITROGEN ABUNDANCE

The N abundance provided by the NI lines is insensitive to the model atmosphere. Secondary indicators – the NH *A–X* system and the CN violet system – confirm the abundance with model HM providing the closest agreement. However, both NH and CN are subject to an unknown error arising from the lack of a definitive determination of the dissociation energies. This problem must be resolved before NH and CN can be accepted as reliable abundance indicators.

The N abundance attributed to the CN violet system (0, 0) and (1, 1) lines is based upon the mean C abundances listed in Section 4.2. An alternative viewpoint would consider the CN analysis to confirm the adopted dissociation energy  $D_0^0 = 7.66$  eV. A high value,  $D_0^0 \sim 7.9$  eV, would be difficult to reconcile with Tables 4 and 5. The CN results also show a modest dependence on the model atmosphere. The weaker  $\Delta v = -1$  sequence and the red system are discussed in Section 4.5.

An abundance  $\log \epsilon(\text{N}) = 7.99$  (models HM and A) is provided by nine *3s–3p* lines. The three *3p–3d* lines give  $\log \epsilon(\text{N}) = 8.11$ . This real discrepancy of 0.12 dex surely reflects the configuration interaction affecting the *3d* terms. The discrepancy vanishes when Richter's

Table 6. Oxygen abundance summary.

Species	Holwegger–Müller			Allen	Vernazza	HSRA	Ayres–Linsky
	log $\epsilon$	$\sigma$	$\Delta_{\text{mic}}$				
[O I] $\lambda$ 6300, 6363	8.92	0.04	0.01	8.88	8.90	8.86	8.88
O I	8.83	0.09	0.02	8.83	8.86	8.80	8.93
OH A–X	8.88	0.15	0.04	8.78	8.78	8.68	8.82

(1961) measured  $f$  values are adopted; an abundance  $\log \epsilon(\text{N}) = 8.09$  fits  $3s-3p$  and  $3p-3d$  lines. In view of the possible uncertainties affecting the absolute scale of the measurements, the N abundance will be based upon the theoretical  $f$  values for the  $3s-3p$  array. Hence,  $\log \epsilon(\text{N}) = 7.99$  is recommended. The uncertainty could be  $\pm 0.10$  dex. The abundance is 0.05 dex larger than the 1968 result. Permitted and forbidden lines of C I and O I appear to yield abundances differing by about 0.10 dex for model H. Perhaps this reflects the effects of departures from LTE and the atmospheric inhomogeneities. Then, a similar correction might apply to the N I lines or  $\log \epsilon(\text{N}) \sim 8.05-8.10$ . Hopefully the inadequacies of NH and CN will be corrected soon.

#### 4.4 THE OXYGEN ABUNDANCE

Two [O I] lines  $\lambda\lambda$  6300, 6363 are the primary indicators of the O abundance. The two lines yield abundances differing by less than 0.03 dex. The abundance is almost independent of the model atmosphere. The mean abundance is  $\log \epsilon(\text{O}) = 8.92$  from models HM and A. The uncertainty is probably less than  $\pm 0.10$  dex. The 0.15 dex increase over the 1968 value is largely attributable to the 5577 Å [O I] line which is excluded from the current line list. Secondary indicators – the O I and OH lines – are consistent with the [O I] lines.

#### 4.5 CNO ABUNDANCES: OUTSTANDING PROBLEMS

If astrophysical demands insist on continued improvement in the accuracy of these important light element abundances, careful attention must be paid to several questions. Many of the improvements are obvious: a uniform use of the high quality photoelectric line profiles; integration of centre-limb studies; re-evaluation of the model atmosphere with an emphasis on improved infrared ( $\lambda < 3 \mu\text{m}$ ) limb darkening observations; evaluation of the effects of solar granulation; continued refinement of the line lists by a detailed attention to weak blends; continued improvements in the  $f$  values; precise determinations of the NH and CN dissociation energies; an accurate  $f$  value for the CN red system (here, dye lasers should be applied), the predicted  $f$  values\* for the (0, 0) band are  $f(0, 0) = 2.6 \times 10^{-3}$  (model HM) or  $1.9 \times 10^{-3}$  (model A) for  $\log \epsilon(\text{C}) = 8.67$ ,  $\log \epsilon(\text{N}) = 7.96$  and  $D_0^0 = 7.66$  eV.

CN presents another spectroscopic puzzle. The weak violet system lines belonging to the  $\Delta v = -1$  sequence (see Section 2.5.3) are markedly stronger than the predicted equivalent widths obtained with the parameters fitting the  $\Delta v = 0$  sequence lines. This might be the signature of a NLTE effect. Examination of the (0, 1) results shows a systematic trend with rotational quantum number. The possibility that the small Franck–Condon factors are subject to a significant rotational dependence is now under close scrutiny.

\* This  $f$  value is to be used with Honl–London factors normalized such that  $S_{J'J''} \approx J$  for  $Q_1$  or  $Q_2$  and  $S_{J'J''} \approx J/2$  for  $P_1, R_1, P_2$  and  $R_2$ . The exact values are to be calculated from the standard expressions.

Additional abundance indicators may be available, e.g. the OH vibration–rotation transitions within the  $X^2\Pi$  state may be detectable near  $3\ \mu\text{m}$  in the photospheric spectrum. OH lines are seen in umbral spectra (Hall 1972) but model atmospheres for umbrae are likely to remain primitive for a long time.

Future studies must scrutinize the LTE assumption. Certainly LTE should be valid for the forbidden lines. Significant departures in the ionization equilibrium for C, N and O are very unlikely. Sedlmayr (1974) has examined the statistical equilibrium of neutral oxygen. A six-level atom was considered with the Holweger (1967) model. This NLTE calculation leads to a reduction of the O abundance with an especially severe effect on the centre-limb variation. At the centre of the disk, the abundance from the 7773 triplet is reduced by about 0.15 dex with respect to the LTE calculation. Weaker lines show abundance decreases of less than 0.1 dex. However, another problem has to be recognized. High-resolution profiles of the O I lines and other high excitation lines are asymmetric. Evidently, the solar atmosphere is inhomogeneous at the depths of formation of these lines. This introduces complications to both the LTE and NLTE analyses.

Preliminary studies of the NLTE effects in molecules (Eugène–Praderie & Pecker 1960; Hinkle & Lambert 1975) suggest that the lines from electronic transitions are formed by scattering so that the source function for weak lines can be equated to an appropriately wavelength averaged mean continuum intensity. Estimates (Hinkle & Lambert 1975) show an abundance increase of about 0.05 dex for weak CH  $A-X$  and  $C_2$  Swan system lines. In the stronger lines, radiative transfer within the lines has to be considered; a prototype NLTE analysis of the strong CN 3883 Å bandhead was reported by Mount & Linsky (1975b). In summary, present indications are that the NLTE effects awaiting discovery appear unlikely to exceed 0.10 dex.

Solar granulation is not explicitly recognized by the five model atmospheres. A two-stream model was included in a preliminary attempt to explore the effects of the granulation. The two-stream model requires the following abundance increases (in dex): the primary indicators: [C I] + 0.10, CH ( $A-X$ ) + 0.06,  $C_2$  + 0.03, N I + 0.03, [O I] + 0.04; some secondary indicators; C I + 0.11, CO = -0.27, NH - 0.13, CN (violet) - 0.16, O I + 0.05, OH + 0.02. As expected, the CN and CO lines show a significant abundance decrease. The primary indicators suggest a systematic abundance increase. A fuller survey of the two- (or multi-) stream concept should be undertaken. The direct approach through examination of spectra of individual granules may soon be possible.

Final recommended abundances are

$$\log \epsilon(\text{C}) = 8.67, \log \epsilon(\text{N}) = 7.99 \text{ and } \log \epsilon(\text{O}) = 8.92$$

and the uncertainty, including the NLTE and granulation contributions is put at 0.10 dex. The abundances provide the ratios (by number of atoms)  $\text{C/O} = 0.56$  and  $\text{N/O} = 0.12$ .

### Acknowledgments

I wish to thank Mr R. Earle Luck and Dr J. G. Collins for assistance with the calculations. Numerous colleagues supplied information prior to publication; I thank the following for especially useful contributions: Drs R. G. Allen, D. Carbon, P. Erman, R. H. Garstang, P. Kjaergaard, E. A. Mallia, L. Testerman, W. L. Wiese. The motivation for this rediscussion of the solar CNO abundances developed out of a discussion with Dr D. C. Morton. This research has been supported in part by the National Science Foundation (Grant AST 75-21803) and the Robert A. Welch Foundation of Houston, Texas.

## References

- Allen, R. G., 1976. In preparation.
- Anderson, R. A. Peacher, J. & Wilcox, D. M., 1975. *J. chem. Phys.*, **63**, 5287.
- Anketell, J. I. & Learner, R. C. M., 1967. *Proc. R. Soc. London A*, **301**, 355.
- Arnold, J. O. & Nicholls, R. W., 1972. *J. quant. Spectrosc. rad. Trans.*, **12**, 1435.
- Arnold, J. O. & Nicholls, R. W., 1973. *J. quant. Spectrosc. rad. Trans.*, **13**, 115.
- Ayres, T. R. & Linsky, J. L., 1976. *Astrophys. J.*, **205**, 874.
- Balfour, W. H. & Cartwright, H. M., 1975. *Can. J. Phys.*, **53**, 1477.
- Balfour, W. H. & Cartwright, H. M., 1976. *Astr. Astrophys. Suppl.*,
- Becker, K. H., Haaks, D. & Tatarczyk, T., 1974. *Chem. Phys. Lett.*, **25**, 564.
- Blackwell, D. E., Ibbetson, P. A., Petford, A. D. & Willis, R. B., 1976. *Mon. Not. R. astr. Soc.*, **177**, 227.
- Blackwell, D. E., Mallia, E. A. & Petford, A. D., 1969. *Mon. Not. R. astr. Soc.*, **146**, 93.
- Brewer, L., Hicks, W. R. & Krikorian, 1962. *J. chem. Phys.*, **36**, 182.
- Brewer, L. & Searcy, A. W., 1956. *A. Rev. Phys. Chem.*, **7**, 259.
- Brooks, N. & Smith, W. H., 1974. *Astrophys. J.*, **194**, 513.
- Brophy, J. H., Silver, J. A. & Kinsey, J., 1974. *Chem. Phys. Lett.*, **28**, 418.
- Brzozowski, J., Bunker, P., Elander, N. & Erman, P., 1976. *Astrophys. J.*, **207**, 414.
- Cameron, A. G. W., 1973. *Space Sci. Rev.*, **15**, 121.
- Carlone, C. & Dalby, F. W., 1969. *Can. J. Phys.*, **47**, 1945.
- Chase, M. W., Curnutt, J. C., Hu, A. T., Prophet, H., Syverud, A. N. & Walker, L. C., 1974. *J. Phys. Chem. Ref. Data*, **3**, 311.
- Cooper, D. M. & Nicholls, R. W., 1975. *J. quant. Spectrosc. rad. Trans.*, **15**, 139.
- Copeland, G. E., 1971. *J. chem. Phys.*, **54**, 3482.
- Corney, A. & Williams, O. M., 1972. *J. Phys. B.*, **5**, 686.
- Crosley, D. R. & Lengel, R. K., 1975. *J. quant. Spectrosc. rad. Trans.*, **15**, 579.
- Curtis, L., Engman, B. & Erman, P., 1976. *Phys. Scrip.*, **13**, 270.
- Danylewych, L. L. & Nicholls, R. W., 1974. *Proc. Roy. Soc. London A*, **339**, 197.
- David, K.-H. & Elste, G., 1962. *Z. Astrophys.*, **54**, 12.
- Delbouille, L., Neven, L. & Roland, G., 1973. *Photometric atlas of the solar spectrum from  $\lambda$ 3000 to  $\lambda$ 10 000*, Institut d'Astrophysique, Liège.
- Desesquelles, J., 1971. *Ann. Phys.*, **6**, 71.
- Elmergreen, B. G. & Smith, W. H., 1972. *Astrophys. J.*, **178**, 557.
- Engleman, R. & Rouse, P. E., 1975. *J. quant. Spectrosc. rad. Trans.*, **15**, 831.
- Erman, P., 1975. *Phys. Scrip.*, **11**, 65.
- Eugène-Praderie, F. & Pecker, J.-C., 1960. *Ann. Astrophys.*, **23**, 622.
- Franklin, J. L., Dibeler, V. H., Reese, R. M. & Krauss, M., 1958. *J. Am. chem. Soc.*, **80**, 298.
- Garstang, R. H., 1956. *The airglow and the aurorae*, p. 324, Pergamon Press, London.
- Gaydon, A. G., 1968. *Dissociation energies and spectra of diatomic molecules*, Chapman and Hall, London.
- German, K. R., 1975a. *J. chem. Phys.*, **62**, 2584.
- German, K. R., 1975b. *J. chem. Phys.*, **63**, 5252.
- Gingerich, O., Noyes, R. W., Kalkofen, W. & Cuny, Y., 1971. *Sol. Phys.*, **18**, 347.
- Goly, A., 1969. *Acta Phys. Polon.*, **36**, 33.
- Grevesse, N. & Sauval, A. J., 1973. *Astr. Astrophys.*, **27**, 29.
- Hall, D. N. B., 1972. *An atlas of infrared spectra of the solar photosphere and of sunspot, umbrae*, Kitt Peak National Observatory.
- Herzberg, G. & Johns, J. W. C., 1969. *Astrophys. J.*, **158**, 399.
- Herzberg, G., Lagerqvist, A. & Malmberg, C., 1969. *Can. J. Phys.*, **47**, 2735.
- Hinkle, K. H. & Lambert, D. L., 1975. *Mon. Not. R. astr. Soc.*, **170**, 447.
- Hinze, J., Lie, G. C. & Liu, B., 1975. *Astrophys. J.*, **196**, 621.
- Hogan, P. & Davis, D. D., 1974. *Chem. Phys. Lett.*, **29**, 555.
- Holweger, H., 1967. *Z. Astrophys.*, **65**, 365.
- Holweger, H. & Müller, E. A., 1974. *Sol. Phys.*, **39**, 19.
- Jackson, W. M., 1974. *J. chem. Phys.*, **61**, 4177.
- Kaskan, W. E. & Nadler, M. P., 1972. *J. chem. Phys.*, **56**, 2220.
- Kernahan, J. A. & Pang, P. H.-L., 1975. *Can. J. Phys.*, **53**, 455.
- Krishnamurty, G. & Narasimhan, N. A., 1969. *J. Mol. Spectrosc.*, **29**, 410.
- Kurucz, R. L. & Peytremann, E., 1975. A table of semiempirical  $f$  values, *Special Rept No. 362*, Smithsonian Astrophysical Observatory.

- Labs, D., 1975. In *Problems in stellar atmospheres and envelopes*, ed. Baschek, B., Kegel, W. H. & Traving, G., Springer-Verlag, Heidelberg, New York.
- Labs, D. & Neckel, H., 1968. *Z. Astrophys.*, **69**, 1.
- Labs, D. & Neckel, H., 1970. *Sol. Phys.*, **15**, 79.
- Labs, D. & Neckel, H., 1971. *Sol. Phys.*, **19**, 3.
- Labs, D. & Neckel, H., 1972. *Sol. Phys.*, **22**, 64.
- Lambert, D. L., 1965. *DPhil thesis*, University of Oxford.
- Lambert, D. L., 1968. *Mon. Not. R. astr. Soc.*, **138**, 143.
- Lambert, D. L., 1971. *Phil. Trans. R. Soc. Lond. A*, **270**, 3.
- Lambert, D. L., Hinkle, K. H. & Mallia, E. A., 1973. *Proc. Conf. Red Giant Stars*, Indiana University.
- Lambert, D. L. & Mallia, E. A., 1974. *Bull. Inst. astr. Czech.*, **25**, 216.
- Lambert, D. L. & Ries, L. M., 1977. *Astrophys. J.*, in press.
- Lambert, D. L. & Swings, J. P., 1967a. *Sol. Phys.*, **2**, 34.
- Lambert, D. L. & Swings, J. P., 1967b. *Observatory*, **87**, 113.
- LeBlanc, F. J., Oldenburg, O. & Carleton, N. P., 1966. *J. chem. Phys.*, **45**, 2200.
- Léna, P., 1968. *Sol. Phys.*, **3**, 28.
- Léna, P., 1970. *Astr. Astrophys.*, **4**, 202.
- Linevsky, M., 1967. *J. chem. Phys.*, **47**, 3485.
- Liszt, H. S. & Hesser, J. E., 1970. *Astrophys. J.*, **159**, 1101.
- Liu, H. P. D. & Verhaegen, G., 1971. *Intl. J. quantum chem.*, **5**, 103.
- Masanet, J., Gilles, A. & Vermeil, C., 1975. *J. Photochem.*, **3**, 417.
- McConkey, J. W., Burns, D. J., Moran, K. A. & Emeleus, K. G., 1966. *Phys. Lett.*, **22**, 416.
- Messerle, G. & Krauss, L., 1967a. *Z. Natur.*, **22a**, 2023.
- Messerle, G. & Krauss, L., 1967b. *Z. Natur.*, **22a**, 1744.
- Meyer, W. & Rosmus, P., 1975. *J. chem. Phys.*, **63**, 2356.
- Miller, M. H., Wilkerson, T. D., Roig, R. A. & Bengtson, R. D., 1974. *Phys. Rev. A*, **9**, 2312.
- Moore, C. E., 1970. *Selected tables of atomic spectra*, NSRDS-NBS3, Section 3.
- Moore, C. E. & Broida, H. P., 1959. *J. Res. nat. Bur. Stand.*, **63A**, 19.
- Moore, C. E., Minnaert, M. G. J. & Houtgast, J., 1966. *Nat. Bur. Stand. Monograph No. 61*.
- Mount, G. H. & Linsky, J. L., 1974. *Sol. Phys.*, **36**, 287.
- Mount, G. H. & Linsky, J. L., 1975a. *Astrophys. J. Lett.*, **202**, L51.
- Mount, G. H. & Linsky, J. L., 1975b. *Sol. Phys.*, **41**, 17.
- Neckel, H., 1975. In *Proceedings of the Workshop on the solar constant and the Earth's atmosphere*, Big Bear Solar Observatory.
- Newkirk, G., 1957. *Astrophys. J.*, **125**, 571.
- Nicolaidis, C. A. & Sinanoglu, 1973. *Sol. Phys.*, **29**, 17.
- Nussbaumer, H., 1971. *Astrophys. J.*, **166**, 411.
- Pierce, A. K., 1954. *Astrophys. J.*, **119**, 312.
- Pierce, A. K., McMath, R. R., Goldberg, L. & Mohler, O. C., 1950. *Astrophys. J.*, **112**, 289.
- Reed, R. I. & Snedden, W., 1958. *Trans. Faraday Soc.*, **54**, 301.
- Richter, J., 1958. *Z. Phys.*, **151**, 114.
- Richter, J., 1961. *Z. Phys.*, **51**, 177.
- Saiedy, F., 1960. *Mon. Not. R. astr. Soc.*, **121**, 483.
- Schaeffer, H. F., 1972. *The electronic structure of atoms and molecules*, Addison-Wesley, Reading, Massachusetts.
- Seal, R. E. & Gaydon, A. G., 1966. *Proc. Phys. Soc.*, **89**, 459.
- Sedlmayr, E., 1974. *Astr. Astrophys.*, **31**, 23.
- Smith, W. H., Brzozowski, J. & Eрман, P., 1976. *J. chem. Phys.*, **64**, 4628.
- Stevens, W. J., 1973. *J. chem. Phys.*, **58**, 1264.
- Stuck, D. & Wende, B., 1974. *Phys. Rev. A*, **9**, 1.
- Stull, D. R. & Prophet, H., 1971. *JANAF thermochemical tables*, 2nd edn (NSRADS-NBS, No. 37).
- Sutherland, R. A. & Anderson, R. A., 1973. *J. chem. Phys.*, **58**, 1226.
- Tipping, R. H., 1976. *J. Mol. Spectrosc.*, **61**, 272.
- Treffers, R. R., 1975. *Astrophys. J.*, **196**, 883.
- Van Rensbergen, W., 1970. *Sol. Phys.*, **11**, 111.
- Vernazza, J. E., Avrett, E. H. & Loeser, R., 1976. *Astrophys. J. Suppl. Ser.*, **30**, 1.
- Yamanouchi, T. & Horie, H. J., 1952. *J. Phys. Soc. Japan*, **7**, 521.
- Young, L. A. & Eachus, W. J., 1966. *J. chem. Phys.*, **44**, 4195.